

## COMPUTATIONAL EVALUATION OF ASSEMBLY TECHNIQUE INFLUENCE ON BALLISTIC PERFORMANCE OF A BULLET – NON-LINEAR RELATION BETWEEN MÉPLAT SIZE AND THE DRAG COEFFICIENT

### ANALIZA NUMERYCZNA WPŁYWU METODY MONTAŻU ELEMENTÓW POCISKU NA CHARAKTERYSTYKI BALISTYCZNE – NIELINIOWA ZALEŻNOŚĆ WSPÓŁCZYNNIKA OPORU OD ŚREDNICY WIERZCHOŁKA

Krzysztof PIASTA<sup>1,\*</sup> , Przemysław KUPIDURA<sup>2</sup> , Jakub MICHALSKI<sup>3</sup> 

<sup>1</sup> Military University of Technology, Faculty of Mechatronics, Armament and Aviation, 2 Sylwestra Kaliskiego Str., 00-908 Warsaw, Poland, e-mail: krzysztof.piesta@wat.edu.pl

<sup>2</sup> Military University of Technology, Faculty of Mechatronics, Armament and Aviation, 2 Sylwestra Kaliskiego Str., 00-908 Warsaw, Poland, e-mail: przemyslaw.kupidura@wat.edu.pl

<sup>3</sup> Military University of Technology, Faculty of Mechatronics, Armament and Aviation, 2 Sylwestra Kaliskiego Str., 00-908 Warsaw, Poland, e-mail: jakub.michalski@wat.edu.pl

\* Corresponding author: krzysztof.piesta@wat.edu.pl

#### Abstract

The continuous development of production and assembly techniques gives rise to the idea of following a new approach in the small-arms ammunition design process. Commonly used intermediate cartridges were designed over 60 years ago, and their construction and assembly processes are not significantly different than what was available almost a century ago. Along with the recent development of individual protection devices and with the general availability of modern ballistic plates utilized in *plate carriers* type of individual armor, it sparks the necessity of designing a new, intermediate cartridge, using new assembly and technology methods. The vital aspect of the ammunition design process is a determination of the materials utilized in bullet elements and its assembly method. Therefore, there is a necessity of evaluating if different assembly techniques can provide the improved ballistic performance of a bullet.

The paper includes a comparison of two differently assembled projectiles with steel penetrators: a standard Full Metal Jacket and a reverse-drawn Semi-Jacketed bullet. The designs were evaluated in terms of their external ballistic performance for specific initial conditions using 2D Computational Fluid Dynamics simulations and, separately, with a semi-empirical method. The paper aimed to assess the influence of the assembly method on the bullet's external ballistic performance. Both calculations revealed a nonlinear relation between the projectile méplat diameter and the coefficient of drag, which indicates a limit where the méplat size reduction is beneficial. The results implicate a perspective bullet construction that would provide the user with better external ballistic performance, more consistent and precise than a standard Full Metal Jacket design.

**Keywords:** mechanical engineering, ballistics, assembly methods, CFD, ammunition.

#### Streszczenie

Nieustanny rozwój technik produkcji i montażu rodzi pomysł wykorzystania nowego podejścia w procesie projektowania amunicji do broni strzeleckiej. Obecnie powszechnie stosowane naboje pośrednie zostały zaprojektowane ponad 60 lat temu, a proces ich wykonania i montażu nie różni się znacząco od technologii dostępnej na początku XX wieku. Biorąc pod uwagę dynamiczny rozwój środków ochrony indywidualnej w ostatnim czasie oraz powszechną dostępność nowoczesnych płyt balistycznych stosowanych w kamizelkach kuloodpornych typu *plate carrier*, zaistniała potrzeba zaprojektowania nowego naboju pośredniego, stosując nowoczesne technologie i metody montażu. Jednym z najistotniejszych aspektów procesu projektowania amunicji jest określenie materiału elementów pocisku oraz sposobu ich montażu, dlatego zasadne jest określenie wpływu metody montażu elementów pocisku na jego właściwości balistyczne.



Artykuł zawiera porównanie dwóch różniących się metodą montażu pocisków z rdzeniem stalowym: standardowego pocisku pełnopłaszczyzowego oraz pocisku półpłaszczyzowego. Konstrukcje zostały ocenione pod kątem ich charakterystyk balistyki zewnętrznej dla określonych warunków początkowych za pomocą symulacji komputerowej dynamiki płynów w 2D oraz niezależnie wykorzystując program balistyczny. Celem pracy była ocena wpływu sposobu montażu elementów na właściwości balistyczne pocisku. Obie metody obliczeniowe wykazały nieliniową zależność między wielkością średnicy wierzchołka pocisku a współczynnikiem oporu, wskazując zakres wartości, do których zmniejszanie rozmiaru wierzchołka jest uzasadnione. Wyniki wskazują perspektywiczną konstrukcję pocisku, która zapewniłaby użytkownikowi lepsze charakterystyki balistyki zewnętrznej, zapewniając lepszą powtarzalność i precyzję niż standardowa konstrukcja pocisku pełnopłaszczyzowego.

**Słowa kluczowe:** inżynieria mechaniczna, balistyka, metody montażu, CFD, amunicja.

## 1. Introduction

The possibility of manufacturing new, before-unavailable shapes of different elements on a wide scale, provides an option of following a new approach in designing small-arms ammunition. The design idea of currently used cartridges has not changed for almost 100 years. Moreover, individual protection devices have significantly improved along with the development of new manufacturing and assembly methods. The general availability of ballistic plates and plate carrier vests has increased, therefore it is becoming standard-issued equipment on the battlefield. Modern individual armor consists of Hard Armour Plates made of ceramic or ultra-high-molecular-weight polyethylene (UHMWPE), and Soft Armour Inserts made of dry Kevlar layers or UHMWPE fabric [1]. It provides complete protection from all intermediate cartridges used nowadays, including the armor-piercing rounds [2]. Therefore, there is an urgent need of providing the NATO soldiers with a cartridge that can defeat the opponent equipped with the aforementioned protection devices, which gives the necessity of evaluating a new projectile in terms of external ballistics.

A typical Full Metal Jacket (FMJ) bullet consists of a lead alloy core and a copper jacket. Usually, the lead-antimony alloy is hot or cold extruded into a wire and cut into slugs. Followingly, the slug is pressed in several punches and formed into the final shape of a core, to fit the inner surface of the ogive closely. Then, the core is fed, seated, and closed into the copper, pointed jacket from the rear part, leaving the base of the bullet open. Boat-tail bullets are then coned and finally closed [3]. Nowadays, projectiles can utilize a steel core inside the copper jacket, filled with a copper slug, instead of a lead core. The assembly method, however, remains similar, with the core fixed through the back of the copper jacket. Such an approach to the design process has its drawbacks and limitations, for instance concerning the shape of the forward part of the bullet: the ogive and méplat, which are vital in the aspect of external ballistics performance. Following a different approach to the main

construction idea may provide the ability to achieve better external ballistic characteristics, greater repeatability, and required armor-piercing abilities of the bullet.

An important reason for further analysis of the materials planned to utilize in a new bullet, is that due to the directives included in regulations of the European Commission on the use of lead in ammunition, toxic-free materials must be used in the new design [4]. The necessity of designing a new, lead-free projectile of improved performance is inevitable.

In a previous analysis, authors have concluded that to achieve the required stopping power while maintaining reasonable peak chamber pressure, a bullet of 6.8 mm diameter would be satisfactory [5]. In terms of the bullet construction, three perspective designs were assessed to be worth analyzing. One construction utilizes a steel penetrator extended from the jacket, assembled from the front. The second is a reverse-jacketed projectile with a light tungsten penetrator extended from a jacket, clasped in an aluminum sleeve, also assembled from the front, and the last design with a tungsten penetrator centered with an aluminum sleeve, but fully jacketed by a copper jacket, assembled in a standard way, from the rear side of the bullet. The main factor differentiating the designs is the choice of assembly direction, creating a Full Metal Jacket or Semi-Jacketed projectile [6].

One of the vital aspects not estimated before is the projectile's ogive shape and méplat diameter. The influence of a differently shaped front part of the bullet on the external ballistics performance was estimated by authors in refs. [7-9]. However, there is still a necessity for analyzing the external ballistic performance of two bullets, with different, before-mentioned assembly methods which provide different possibilities of the méplat dimensions. The main objective of the paper is an estimation of the méplat diameter influence on the aerodynamics of a bullet, to assess which design idea is more perspective.

## 2. Material and methods

The following constructions were analyzed:

- 6.8 mm Full Metal Jacket Steel Core (FMJ SC);
- 6.8 mm Semi-Jacketed Steel Core (S-J SC).

The bullets are characterized by equal mass and overall external shape, with a difference concerning only the diameter of a méplat. Different variations of méplat size were analyzed to assess its influence on the drag coefficient.

### 2.1. 6.8 mm FMJ Steel Core

The first design is a standard Full Metal Jacket bullet with a steel core. The projectile assembly requires forming the steel core, then, inserting the core into the copper jacket from the rear part, filling the space with a copper slug and enclosing the jacket, precisely shaping the ogive, méplat and boattail. The base of the bullet in that case remains open. Currently used intermediate FMJ bullets with the standard manufacturing and assembly methods provide a méplat diameter of 1.0 mm up to 1.6 mm. The design of analyzed construction is shown in Fig. 1.

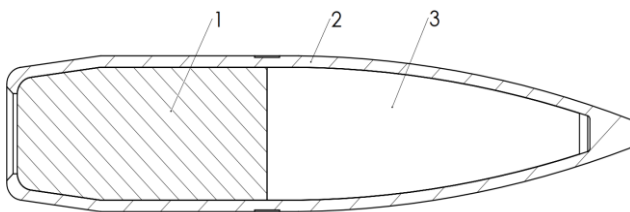


Fig. 1. Cross section of 6.8 mm FMJ Steel Core bullet  
1 – copper slug, 2 – copper jacket, 3 – steel penetrator

### 2.2. 6.8 mm Semi-Jacketed Steel Core

The second construction is a Semi-Jacketed projectile, with a steel arrow-shaped penetrator exposed from the copper jacket. The bullet is assembled from the front part of the jacket, while the copper slug is formed and inserted into the drawn copper jacket and the steel arrow-shaped penetrator is inserted in the jacket and enclosed in it.

The following design provides greater possibilities in terms of precision and consistency of the ogive and méplat dimensions. Therefore, concerning the possibility of manufacturing a steel penetrator shape, designs with méplat diameters of 0.8 mm, 0.6 mm and 0.4 mm were analyzed. The projectile is shown in Fig. 2.

Dimensions and data of the projectiles are shown in Table 1.

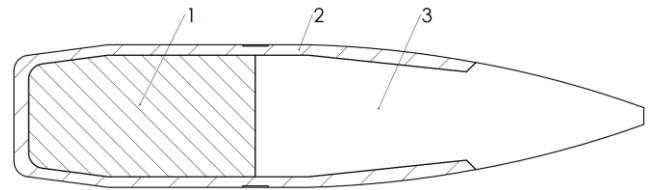


Fig. 2. Cross section of 6.8 mm Semi-Jacketed Steel Core bullet  
1 – copper slug, 2 – copper jacket, 3 – steel penetrator

Table 1. Technical data of designed bullets

Parameter	Value
Bullet length (mm)	30
Bullet mass (g)	6.6
Steel core mass: FMJ/S-J (g)	2.04/2.32
Ogive radius (mm)	50
Méplat diameter (mm)	0.4, 0.6, 0.8, 1.0, 1.2, 1.4, 1.6

## 3. Calculation

Two separate approaches were followed to estimate the performance of designed projectiles. Numerical approach, performing Computational Fluid Dynamics analysis with ANSYS Fluent software, and a semi-empirical approach, through simulations with PRODAS software. For each projectile several calculations were performed, varying the méplat diameter, with all the remaining dimensions preserved.

### 3.1 Numerical approach

Ansys Fluent 2022R2 was used to perform the numerical calculations. The software solves Reynolds-Averaged Navier-Stokes equations using the finite volume method.

#### 3.1.1. Geometry and domain

2D geometries representing the external shape of the projectiles and surrounding domains were designed using the Design Modeler component of Ansys 2022R2. Separate geometries were designed for each méplat diameter size: 0.4 mm, 0.6 mm, 0.8 mm, 1.0 mm, 1.2 mm, and 1.4 mm. To ensure resolved wake flow, the size of the domain was set to approximately 30 diameters radially away from the bullet, 17 diameters forward, and 23 diameters rearwards.

Using Ansys Meshing structured, quadrilateral meshes were created. The vicinity of the projectile surface is presented in Fig. 3. Discretization parameters for each calculation are presented in Tab. 2. The non-dimensional distance from the wall to the first mesh node ( $y^+$  value), should be of the order of 1.0 to correctly resolve the flow in the boundary layer. For all analyzed velocities the  $y^+$  value was maintained lower than 1.0 through the projectile's whole surface,

and less than 0.5 around the base and boattail, to allow a correct solving of the wake flow [10].

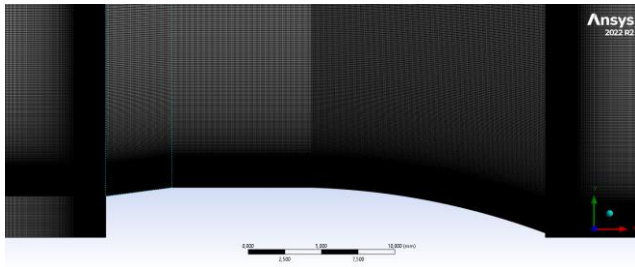


Fig. 3. Mesh generated in proximity of the geometry

Table 2. Discretization scheme parameters and mesh metrics

Parameter	Value
Number of elements	1506800
First cell height (μm)	< 0.44
Max. skewness	0.225
Max. aspect ratio	2604
Min. orthogonal quality	0.933

### 3.1.2. Simulation settings

Steady-state, 2D axisymmetric, double-precision, density-based solver was initiated for the analysis of external compressible flow. The value of zero-yaw drag coefficient is negligibly different for unsteady and steady-state calculations [11], therefore there is no need to follow a computational power demanding unsteady approach. To obtain several values of drag coefficient for each different méplat size, simulations were performed for the steady-flow velocities of Mach 1.5, 2.0, and 2.5, where the latter corresponds to the assumed muzzle velocity of 850 m/s.

In order to model the turbulence in the flow correctly, a viscous model of  $k-\omega$  SST with compressibility effects was chosen. The ideal-gas settings were applied with the viscosity model set to Sutherland [12]. For each simulation, the boundary conditions shown in Table 3 were set. Simulations were initiated using the implicit, First Order Upwind approximation algorithm method, with Roe-FDS flux type and Courant number equal to 0.8. After convergence with the initial solution, the Second Order precision algorithm was followed.

Table 3. Boundary conditions set for the analysis

Boundary	Type
Inlet	Pressure-far-field
Outlet	Pressure-outlet
Axis	Axis
Projectile	Wall (no-slip)
Far-field	Pressure-far-field

Convergence criteria were set of residuals to reduce at least 3 orders of magnitude and the drag coefficient changing less than 0.001 over 500 iterations. The determining factor for all the cases was the change in the drag coefficient value. The solution has converged after approximately 16000 iterations for the velocity of Mach 2.5 and 2.0, and around 25000 iterations for Mach 1.5. Figure 4 presents the residual reduction for the Mach 2.5 case of 1.2 mm méplat diameter simulation. A peak in the values is noticeable after 7000 iterations, due to the discretization theme order change from 2<sup>nd</sup> to 1<sup>st</sup>.

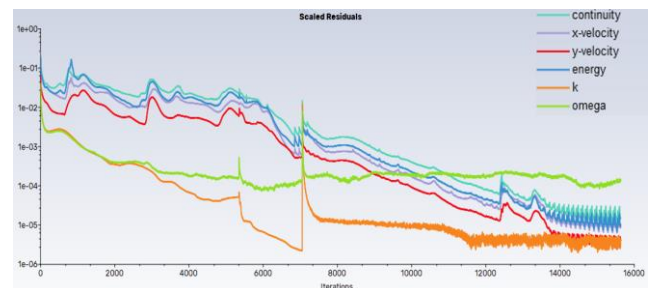


Fig. 4. Residuals behavior (Méplat dia.: 1.2 mm, Mach 2.5):

### 3.2. Semi-empirical approach

Using the PRODAS V3.5 Arrow Tech software, semi-empirical calculations of the projectiles were performed. Geometries of the projectiles were designed (Fig. 5, Fig. 6), with méplat diameter sizes varying from 0.4 mm to 1.6 mm.

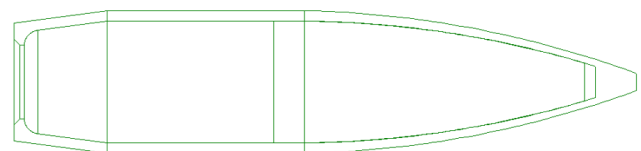


Fig. 5. Prodass geometry of the 6.8 mm FMJ SC projectile

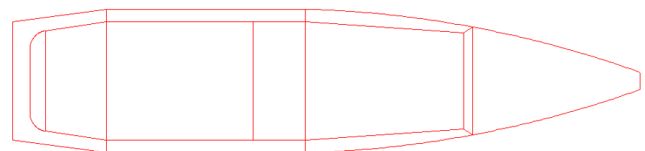


Fig. 6. Prodass geometry of the 6.8 mm S-J SC projectile

To validate the models, stability evaluation was performed, and the results indicated that all the projectiles are characterized by a gyroscopic factor (GF) of over 4.0. For uncertainties of the muzzle velocity, mass distribution and atmospheric conditions, the required GF value should exceed 1.5, therefore the estimation confirmed that the projectiles

are characterized by good stabilization with uncertainties safety margin [13].

To compare the trajectories of designed projectiles, point-blank shooting simulations were performed. The following initial conditions were set [14]:

- muzzle velocity:  $v_0 = 850$  m/s;
- target height:  $h = 0.5$  m;
- barrel length:  $l = 406$  mm;
- barrel twist:  $l_0 = 178$  mm, 6 grooves;
- pressure:  $P_0 = 1013.2$  hPa, temperature:  $t = 15^\circ\text{C}$ , air density:  $\rho_0 = 1.225$  kg/m<sup>3</sup>, speed of sound:  $v_s = 340.2$  m/s.

## 4. Results

### 4.1. Computational Approach

#### 4.1.1. Flow fields

Velocity magnitude fields for the 1.2 mm méplat projectile are shown in Fig. 7. The flow behaviors are practically identical for the remaining cases.

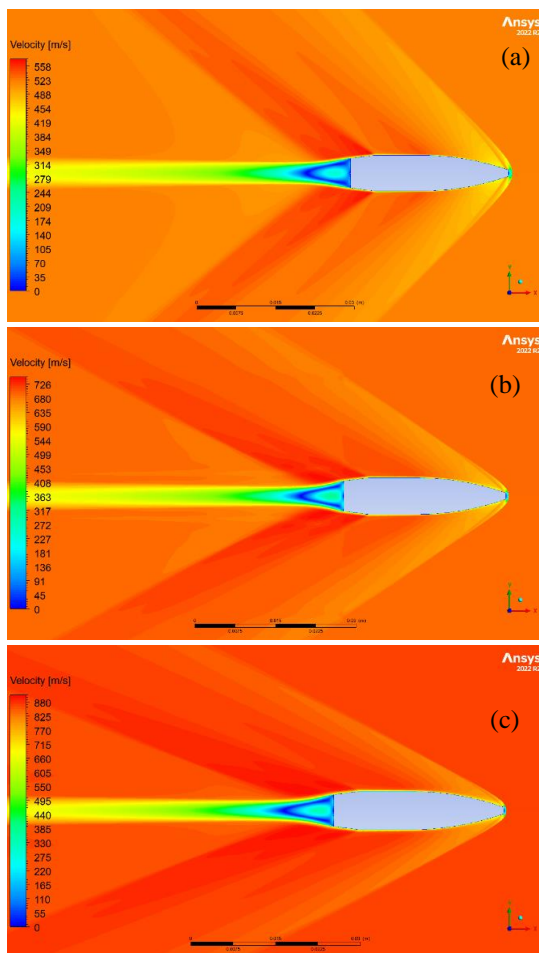


Fig. 7. Velocity fields (méplat dia. 1.2 mm): (a) Mach 1.5, (b) Mach 2.0; (c) Mach 2.5

In the case of Mach 1.5 (Fig. 7a), the flow is supersonic through the whole surface of the projectile,

except for the base region and a small local subsonic region in the vicinity of the blunt nose. The bow shock can be noticed close to the projectile nose with a standoff of approximately 0.5 diameters. The standoff decreases and the curvature of the shock increases with the flow velocity, becoming oblique in Mach 2.0 (Fig. 7b). Furthermore, a trailing shock is visible at the end of the boattail, with a region of very low flow velocity magnitude and pressure at the base of the projectile, which corresponds to the base drag, and increases with the flow speed. In the case of high supersonic velocity of Mach 2.5 (Fig. 7c), the oblique shock angle is even smaller, and the shock wave appears to be almost in contact with the projectile's méplat.

Fig. 8-10 present the nose region for different méplat diameters, in the case of Mach 2.0.

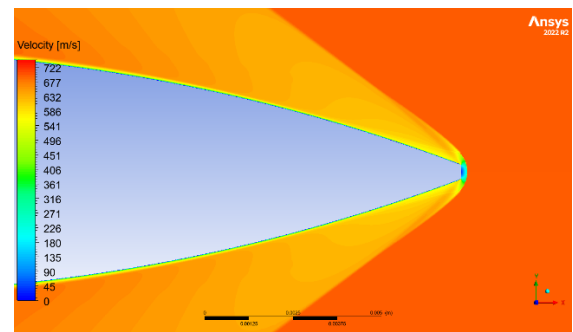


Fig. 8. Velocity field in nose region – méplat dia.: 0.4 mm, Mach 2.0

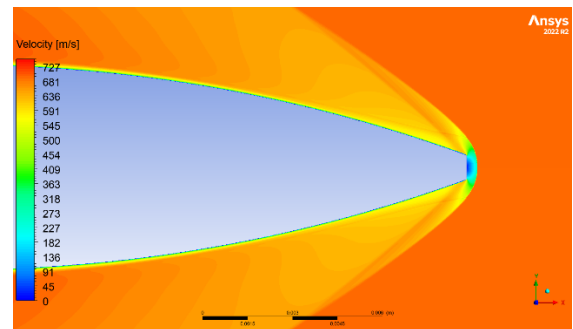


Fig. 9. Velocity field in nose region – méplat dia.: 0.8 mm, Mach 2.0

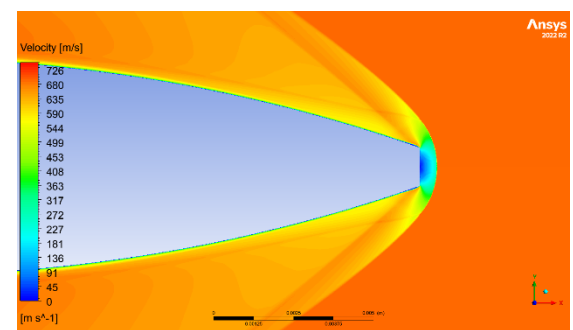


Fig. 10. Velocity field in nose region – méplat dia.: 1.2 mm, Mach 2.0

The diameter of the méplat directly influences the behavior of the shock wave. The increase in méplat diameter results in an increase of the bow shock standoff from the projectile. The local nose subsonic region is noticeably larger with a larger méplat diameter.

#### 4.1.1. Drag coefficient

The calculated drag coefficient values for different flow velocities and méplat diameters are presented in Table 4 and Fig. 11.

Table 4. Calculated drag coefficient – numerical approach

Mach number	Méplat diameter (mm)					
	6.8 mm S-J SC			6.8 mm FMJ SC		
	0.4	0.6	0.8	1.0	1.2	1.4
1.50	0.354	0.354	0.348	0.351	0.353	0.358
2.00	0.300	0.301	0.302	0.304	0.318	0.318
2.50	0.276	0.276	0.273	0.272	0.284	0.290
AVG	0.310	0.310	0.308	0.309	0.318	0.322

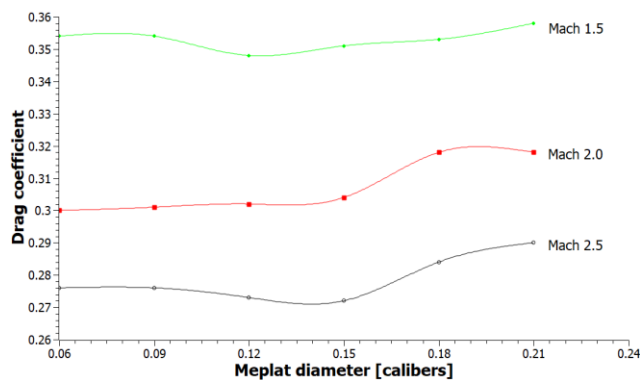


Fig. 11. Calculated drag coefficient versus méplat diameter (numerical results)

The results indicate a non-linear relation between the méplat diameter and drag coefficient. For a set ogive length, the value of drag force reduces with the reduction of a méplat to a certain value. Further reduction of the diameter causes an increase, or at maximum a lack of reduction in the drag coefficient value (case of Mach 2.0). In analyzed case of a 6.8 mm bullet, the lowest drag coefficient of 0.308 was achieved with a méplat size of 8.0, which equals 0.12 calibers. However, the differences between 0.4 mm and 0.8 mm meplat are negligible and can be considered within the calculation error.

### 4.2. Semi-empirical approach

#### 4.2.1. Projectiles trajectories

Point-blank trajectories calculated with the semi-empirical approach are shown in Fig. 12 below.

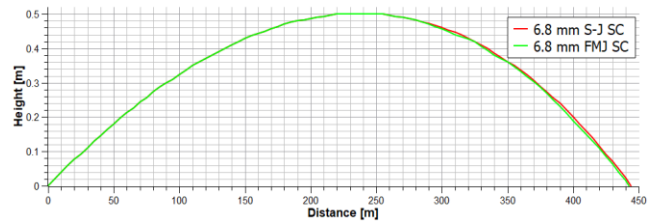


Fig. 12. Point-blank trajectories

There is a slight difference in the point-blank range between analysed projectiles. The 6.8 mm FMJ SC achieves 442.6 m of point-blank range at 850 m/s to a 0.5 m high target, while the 6.8 mm S-J SC equals 444.1 m. The difference of less than 0.4 % however, is negligible.

#### 4.2.2. Drag coefficient

Drag curves calculated with a semi-empirical method for the projectiles 6.8 mm S-J SC with 0.8 mm méplat diameter and 6.8 mm FMJ SC with 1.2 mm méplat are shown in Fig. 13 below.

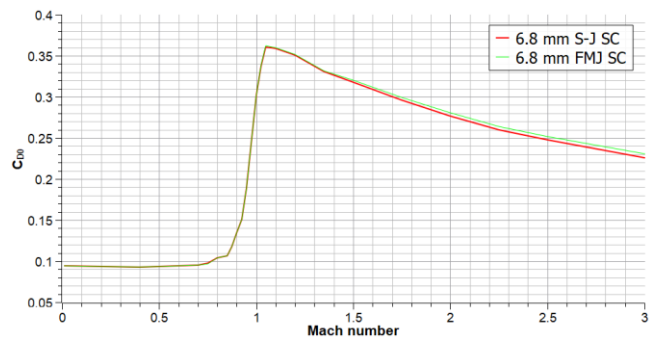


Fig. 13. Calculated drag curves of the projectiles

As assumed, due to the almost identical external shape of the designs, with slight variations of the méplat diameter, the drag curves of the projectiles closely coincide. However, in the high supersonic range, the 6.8 mm S-J SC projectile is characterized by a slightly lower coefficient of drag, reaching 0.248 at Mach 2.5, compared to 0.250 for the FMJ.

The values of the drag coefficient calculated for each méplat size and different Mach numbers are presented in Table 5 and graphically in Fig. 14.

Table 5. Calculated drag coefficient – semi-empirical approach

Mach number	Méplat diameter (mm)					
	6.8 mm S-J SC			6.8 mm FMJ SC		
	0.4	0.6	0.8	1.0	1.2	1.4
1.50	0.322	0.319	0.318	0.319	0.320	0.324
1.75	0.301	0.298	0.296	0.298	0.299	0.305
2.00	0.282	0.279	0.277	0.278	0.280	0.287
2.25	0.266	0.263	0.260	0.262	0.264	0.272
2.50	0.254	0.251	0.248	0.250	0.252	0.261
AVG	0.285	0.282	0.280	0.281	0.283	0.290

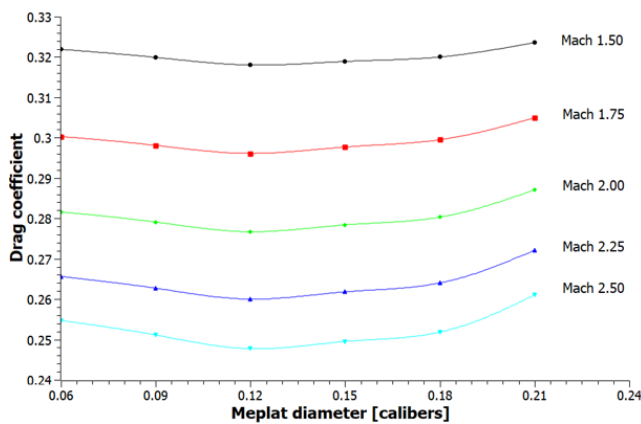


Fig. 14. Calculated drag coefficient versus méplat diameter (semi-empirical approach)

The value of the drag coefficient decreases with the decrease of bullet méplat diameter down to 0.8 mm – 0.12 diameters. The values are lower than achieved with the numerical method, averaging 0.280 for a 0.8 mm diameter. However, both simulations confirm the tendency of achieving the lowest drag with a méplat diameter of approximately 0.12-0.15 calibers.

#### 4. Discussion

The main aim of the paper was to assess the relation between the méplat size of a bullet and the coefficient of drag, to assess a better assembly method for a perspective construction. The characteristics were evaluated with two separate methods, and the results indicate similar conclusions.

Drag dependence of méplat diameter in calibers shown in Fig. 11 and Fig. 14 indicate that there is an improvement in terms of the external ballistic performance of a bullet while reducing the méplat to a value of 0.10-0.15 diameters. Further reduction not only does not decrease the drag acting on a projectile but may even increase it for certain cases. The reason behind this effect might be the wave drag differences due to a different angle between the ogival part of the projectile and the flow direction, which increases with the decrease of the méplat diameter when the ogive length remains unchanged. Charts in Fig. 11 and 14 show that with the increase of the flow velocity, the non-linear relation is stronger – the drag decreases and increases more rapidly at the vicinity of its minimum value for Mach 2.5 than Mach 1.5 and 2.0, which confirms the wave-drag effect explanation. Therefore, in cases of assumed high supersonic bullet flow, the importance of precise and consistent méplat dimensions increases. The relation between the méplat diameter and coefficient of drag value confirms the theory presented in ref. [7].

The use of CFD methods in the estimation of the ballistic characteristics of a bullet is more time and

computationally expensive, however, it provides accurate results. Simulations estimated the value of zero-yaw drag coefficient, as well as the velocity, pressure, and density changes in the fluid, providing the ability to analyze the behavior of air in proximity to the projectile surface. On the other hand, utilizing PRODAS ballistic software provides quick, cost and time-effective results by comparative analysis of the design to a considerable amount of actual rounds data. It is a less accurate method than a CFD analysis, however, it can be a very valuable tool, when used in terms of a preliminary analysis.

#### 5. Conclusions

- To reduce the drag force acting on a 6.8 mm projectile in flight, in case of a set ogive length, a méplat diameter of between 0.8 mm to 1.0 mm should provide the best outcome. Achieving that value with higher precision and repeatability is possible with steel element, so with the reverse-drawn semi-jacketed design of a projectile;
- Designing a bullet with a steel front part provides additional benefits, like increased resistance to damage due to transport, carrying, and weapon operational cycle, which means more consistent performance of the ammunition;

Analyzing the material properties of the designed construction, the following hypothesis can also be stated:

- Semi-jacketed bullet would provide increased terminal ballistics performance, due to a harder material being in immediate contact with the target;
- Design with a steel penetrator outside of the jacket would help to avoid the material wrinkling at the projectile nose due to the lubrication, which causes imbalances and therefore stability issues and is common for standard copper jacketed bullets production;
- Two-material ogival part of the bullet provides the possibility of designing a hybrid ogive shape, with a secant front – steel penetrator shape, turning into a tangent shape of the jacketed part, which would be a further increase in repeatability and constant external performance.

Results from this study provide valuable information concerning the design process of a projectile, in terms of the technique of assembly and the necessity of precision of the bullet's front part. The main conclusion is that the drag dependence on méplat diameter is not constant – reducing the méplat size reduces the coefficient of drag to some point, after

which further diameter reduction is not needed, or even undesirable for certain flow velocities.

The results have strong implications for future bullet designs. Further works should focus on analyzing the projectile external performance dependence on minor damage caused during production and assembly, which may cause irregularities and asymmetries.

### Acknowledgements

The work was financed by Military University of Technology under research project UGB 22 829.

### References

1. Crouch G. I. 2021. "Defence Technology". *Critical interfaces in body armour systems* 17 (6): 1887-1894.
2. NIJ. 2000. *Resistance of Personal Body Armor NIJ Standard-0101.04*, Washington: U.S. Department of Justice, Office of Justice Programs.
3. Frost George. 1990. *Ammunition making*. Washington: National Rifle Association.
4. Official Journal of the European Union. 2021. COMMISSION REGULATION (EU) 2021/57 of 25 January 2021.
5. Piasta Krzysztof, Przemysław Kupidura and Grzegorz Leśnik. 2022. "Projectile for a New Intermediate Cartridge", *Problems of Mechatronics. Armament, Aviation, Safety Engineering* 13 (4) : 123-126.
6. Piasta Krzysztof, Przemysław Kupidura. 2023. "Perspective Armour Piercing intermediate Cartridge Projectile", *Problems of Mechatronics. Armament, Aviation, Safety Engineering* 14 (1) : 89-104.
7. McCoy Robert L. 2012. *Modern exterior ballistics, Revised 2<sup>nd</sup> Edition*. USA: Schiffer Military, s. 32-34, 71.
8. Muruganatham, V. R., Thoma Babin. "Numerical investigation of hybrid blend design target bullets", MATEC Web of Conferences 172 01006.
9. Larson, Eric, Racha Lwali and Dejan Samardzic. 2015. "Bullet Drag Estimation with Compressible Conical Flow Equations and Commercial Software", Department of Aerospace Engineering and Engineering Mechanics, San Diego State University research.
10. Rodriguez Sal. 2019. *Applied Computational Fluid Dynamics and Turbulence Modeling*. Switzerland: Springer Nature, s. 238.
11. DeSpirito James, Karen Heavey. 2004. "CFD Computation of Magnus Moment and Roll-Damping Moment of a Spinning Projectile", AIAA 2004-4713.
12. Ansys Inc. 2021. *Ansys Fluent Theory Guide*. USA: Ansys Inc.
13. Litz Bryan. 2015. *Applied ballistics for long-range shooting*. USA: Applied Ballistics LLC, s. 157-162.
14. Arrow Tech. *Prodas V3 Documentation*.